

Viscoelastic Properties of Single Proteins using Small Amplitude AFM

A Thesis

submitted to

Indian Institute of Science Education and Research Pune
in partial fulfillment of the requirements for the
BS-MS Dual Degree Programme

by

Saurabh Talele

20121079




April, 2017

Supervisor: Dr. Shivprasad Patil
Indian Institute of Science Education and Research Pune

© Saurabh Talele 2017
All rights reserved

Certificate

This is to certify that this dissertation entitled Viscoelastic Properties of Single Proteins using Small Amplitude AFM towards the partial fulfilment of the BS-MS dual degree programme at the Indian Institute of Science Education and Research, Pune represents study/work carried out by Saurabh Talele at Indian Institute of Science Education and Research under the supervision of Dr. Shivprasad Patil, Associate Professor, Department of Physics, during the academic year 2016-2017.


30/03/2017
Dr. Shivprasad Patil

Committee:

Dr. Shivprasad Patil

Dr. Arijit Bhattacharya

This thesis is dedicated to my grand parents

Declaration

I hereby declare that the matter embodied in the report entitled Viscoelastic Properties of Single Proteins using Small Amplitude AFM are the results of the work carried out by me at the Department of Physics, Indian Institute of Science Education and Research under the supervision of Dr. Shivprasad Patil and the same has not been submitted elsewhere for any other degree.


30/3/2017
Saurabh Talele

Acknowledgments

My first thanks goes to the current and the past members of my lab. It has been a wonderful experience and I will never forget the three years I spent with the good people of this lab. This project would not have been possible without Ajith, Shatruhan, and Amandeep and I owe them much more than a Thanks. I would especially like to thank the physics department technical support team, Nilesh sir and Prashant sir, they helped me solve technical problems which would have taken weeks for me to figure out had they not helped me. Special thanks to Dr. Koti from TIFR, Mumbai for providing us the protein plasmid samples.

I thank my parents and my sister who constantly supported me with their trust and love. I thank my friends who made my time at IISER a memorable one.

Finally and most importantly, I would like to thank my guide Dr. Shivprasad Patil for giving me the opportunity to work on this wonderful project. We have had exciting discussions and I have learnt a lot from him. Thank you Sir !

Abstract

This project is about construction of a Home-Built small amplitude Atomic Force Microscope and measuring the viscoelastic response of unfolding proteins at single molecule level. There are very few techniques to quantify the stiffness and the dissipation in single protein molecules. This AFM uses a highly sensitive fiber optic based interferometric detection mechanism to detect changes in cantilever amplitude as low as 0.5 pico meters. This instrument is an enhanced force spectroscopy tool built to measure the local stiffness and dissipation in single proteins. The project focuses on dynamic force spectroscopy measurements on titin I27 polyprotein constructs. The measured stiffness is found to be of the order of $\sim 10^{-4}$ N/m dissipation is of the order of $\sim 10^{-9}$ kg/s, which compares well with other methods and is well below the upper bound that has been estimated from a non-observation in commercial Atomic Force Microscopy set-up. The technique holds promise for probing the energy landscape directly and in a single pass measurement. In this thesis, I will discuss the historical perspective, the preliminaries for the study, the construction of the instrument, the experiments and the findings of the single molecule unfolding studies using this the Small Amplitude AFM.

Contents

Abstract	xi
1 Introduction	1
1.1 The history	1
1.2 Towards Protein	2
1.3 The Instrument	6
2 Theory	7
2.1 Atomic Force Microscopy	7
2.2 Oscillator Models for Cantilever	11
3 Methods	15
3.1 The Instrument	15
3.2 Experimental	29
4 Results	31
4.1 Measurement and Data Analysis	31
4.2 Noise analysis	34
5 Discussion	37

5.1	Origins of Elasticity and Dissipation in Proteins	37
5.2	Thermodynamics of Protein Function	38
5.3	Future Plans	40

Chapter 1

Introduction

This chapter provides an introduction to the project covering the historical aspects, literature survey of methods and motivation for this project.

1.1 The history

Humans have always been fascinated by the very phenomenon of life. The fundamental question of ‘what is life?’ however, remains unanswered after over 2 millennia of philosophical debate between great thinkers who have attempted to define life. Aristotle (350 BC) viewed life as a fundamental property of nature, Descartes (1596) saw life as a mechanism involving interacting matter, Kant (1724) took this idea further and called life as an organization of processes and Weber (1864) saw life as an emergent property arising out of highly complex systems[1].

It was not much later that physicists engaged in to give a new approach to our understanding of life. In 1943, Erwin Schrödinger in his lecture series ‘What is Life?’ at Dublin Institute for Advanced Studies presented his views on the thermodynamics of living things. He talked about how living things must generate order from disorder through some processes in order to continue living[1, 2]. Later, physicists like Prigogine, Morowitz, and Bernal helped develop this idea further concluding that the cell is an open system and can be well-understood using non-equilibrium thermodynamics. By this time, many scientists

like Karl Pearson, Helmholtz and Carl Ludwig also had developed approaches to understand biological phenomena using physics and mathematics[3]. Pearson referred to this new interdisciplinary methodology of science as Biophysics.

Biophysics aims at understanding complex life processes using the simple laws of physics and mathematics. A quantitative way to understand life is to learn how living systems work rather than trying to define life itself. The early twentieth century saw a large number of discoveries in biology owing to advancements in optical microscopy. In late twentieth century, the invention of techniques such as Scanning Electron Microscopy, Fluorescence Confocal Microscopy, and Atomic Force Microscopy gave new dimensions to the ongoing research. New techniques continue to be developed and old ones are improvised to discern the complexity of life processes. Some of the current questions in the field of Biophysics are; how does the molecular machinery work inside living cells? How do nerve cells communicate? And how do cells sense their physical surroundings?

1.2 Towards Protein

One of the astounding topics of interest for biophysicists is proteins. These biomolecules are long chains of amino acids that carry out most of the functions (enzymatic, signaling, structural) within a cell. To carry out its function, a protein must acquire a specific 3-dimensional structure. The process by which this linear chain of amino acids transforms into a 3D structure is called *folding*. Harriette Chick and C. J. Martin first observed this phenomenon in 1910 and reported in their paper that the precipitation of protein was followed by *denaturation*, in which protein became less soluble and more chemically active[4]. In 1924, Anson proposed that denaturation was a reversible process[5], which was initially made fun of referring it to 'unboiling an egg' but was experimentally confirmed by Chris Anfinsen in 1960[6]. Anson also proposed that the denaturation was a two-state process and that the free energy change was very little as compared to typical chemical reactions. Hsien Wu (1929) suggested that this process was purely a physical conformation change not involving any chemical reactions referring to the low free energy change[7]. This 'thermodynamic hypothesis' suggested that a protein folds into a stable final state which represents the global minima of free energy of the molecule.

1.2.1 The Protein Folding Problem

An immediate question that one thinks of is that how exactly does a protein molecule reach the global minima in the free energy? or in other words, what is the mechanism of protein folding? This question is broadly referred to as The Protein Folding Problem. The problem is composed of three important questions[8] :

1. What is the physical code by which an amino acid sequence dictates it's native 3D folded structure?
2. How can proteins fold so fast? (Levinthal's paradox).
3. What determines the stability and activity of the folded protein?

The first question is self-explanatory and is about understanding how the amino acid chain interacts with the surroundings to result in the native folded structure. The second question is about the speed of folding. In 1968 Levinthal raised the question of how, despite an astronomically large number of conformations available to it, the protein chain can fold into its native state so quickly (within microseconds to milliseconds). While a random search through all the configurations would take more time than the age of the universe, How does the protein know what conformations not so to search? And this is known as Levinthal's paradox[8]. Experimental results hint in the presence of folding intermediates, which are partially structured states along the 'folding pathway'. The third question deals with the dynamic properties of folded proteins. The Energy landscape of the protein is hypothesized as being a funnel-like where a protein starts as a random chain, takes incremental steps downhill towards the global minima, and thus, traverses the landscape. However, the landscape that might look smooth globally can have local roughness and saddle points, which might end up causing the chain to misfold. In living organisms, misfolded proteins cause dangerous diseases like Alzheimer's and Parkinson's disease.

1.2.2 Experimental Approaches

Determining the energy landscape is important to understand various aspects of protein folding and dynamics. The experimental methods used for probing the energy landscape

are based on the fact that protein folding is a reversible process. Hence, the experiments involve controlled unfolding (denaturation) using temperature, pressure or chemicals like urea to unfold a protein. The trajectory followed by the protein molecule is projected on a reaction coordinate defined by the temperature, pressure or chemical concentration. To observe the response of a protein, methods such as FRET, Cryo-electron microscopy, Circular Dichroism and NMR are used. These methods, however, are bulk measurements and probe only the average behavior of a large number of molecules. Thus, it is difficult to resolve simultaneously occurring (un)folding pathways or folding intermediates as the molecule traverses the multidimensional energy landscape [9].

After the invention of the Atomic Force Microscope by Binning et.al in 1986, it immediately found its application in force spectroscopy techniques for studying protein unfolding developed in 1990's by Carlos Bustamante[10], Hermann Gaub[11], and Matthias Reif. AFM provides a novel method of studying protein folding in which mechanical force acts as the denaturant, which can potentially give new insights into protein folding process and energy landscapes. The AFM differs from the conventional bulk methods primarily in three ways[12].

1. It is a single molecule method, which makes it possible to observe differences in the nature of unfolding from molecule to molecule.
2. The response of the protein to the external force can be mapped onto a well-defined reaction coordinate namely, the end-to-end extension of the molecule.
3. It offers the possibility of probing alternative regions or folding intermediates of the energy landscape, which is impossible to do in bulk experiments.

Since we have a method of using external force as a denaturant, we can address questions like how proteins resist external mechanical stresses? What is the origin of mechanical strength of a protein molecule? Do proteins unfold by the same pathway under force as they do physiologically? In 1997, H.Gaub reported the unfolding of titin protein at single molecule level[11]. titin is a multi-domain muscle protein that is observed to be under mechanical stress in the muscle cells. It is recognized by its characteristic repeated sawtooth-like unfolding in the force versus extension plots. To probe the energy landscape of a protein, we need to measure its mechanical response in terms of the elastic and dissipative contributions to the

transition from folded to unfolded state. Additionally, measuring the viscoelastic response of the molecule also tells us about the dynamics of hopping between closely spaced local minima in the folding funnel[13].

A simple approach to measure the elastic and dissipative properties is to provide sinusoidal oscillations to the cantilever and measure the amplitude and phase at every point during a force spectroscopy experiment. People have measured the dynamic responses of polysaccharides (Humphris et al., 2000)[14], synthetic polymers (Kienberger et al., 2000)[15], nucleic acids (Liu et al., 1999), receptor-ligand complexes (Chtcheglova et al., 2004)[16], and proteins (Mitsui et al., 2000; Okajima et al., 2004)[17]. These methods determine the dynamic properties by using the amplitude and the phase data into linear models of forced damped harmonic oscillators. However, it is found that there are fundamental problems with this simple-looking approaches.

1. The signal to noise ratio in these single molecule experiment is limited by the deflection detection sensitivity of the AFM.
2. These techniques involve oscillating the cantilever at the resonance frequency in order to maximize the amplitude and hence the signal to noise ratio. This leads to the cantilever amplitudes as high as 10 nm. Typically, the range of intermolecular forces is around 2-3 nm thus, probing these short-ranged interactions with larger amplitudes results into highly nonlinear cantilever dynamics and the linear harmonic oscillator model of the cantilever doesn't hold.
3. Soft cantilevers of low spring constant values are used in order to maximize the change in amplitude making it more susceptible to thermal noise.

The solutions for these problems are in principle, straightforward.

1. In order to avoid the non-linear behavior, one should reduce the excitation amplitude to over one magnitude below the range of interaction forces.
2. One can drive the cantilever at off-resonance frequency where the amplitude is lower and phase lag is negligible.
3. To combat the low signal to noise ratio, one can develop a highly sensitive detection system.

1.3 The Instrument

The solutions stated above are difficult to implement in commercial AFMs mainly because of the low deflection detection sensitivity of the laser deflection systems. Thus, one cannot go down to lower amplitudes without compromising the signal to noise ratio in the measurement. Off-resonance measurements in commercial AFMs is also a problem since it uses weak (low stiffness) cantilever however, weak stiffness also increases thermal noise and hence one needs to use cantilevers with high stiffness which commercial systems once again fail at due to their low deflection detection sensitivity. Thus, in order to study the viscoelastic properties of single proteins, one has to develop a highly sensitive deflection detection mechanism.

In this project, we introduce a Homemade Small Amplitude Atomic Force Microscope which uses an optic fiber based interferometer to detect cantilever deflection. The setup is derived from the one used by Patil and Hoffmann (2005)[18]. The interferometer is Fabry-Perot type and gives sensitivity that is hundred times higher than the commercial quadrant photodiode based detectors. This setup allows us to detect amplitudes as low as 5 pm, allowing us to perform dynamic force spectroscopy at truly off-resonance and low amplitudes that ensure the validity of the linear harmonic oscillator models.

We use this instrument to study the mechanical unfolding of titin I27 polyprotein constructs having seven identical domains in tandem which was synthesized from a plasmid using the standard procedure. We use two models for analysis namely the point-mass model and a recently reported continuous beam model of the cantilever to determine the viscoelastic parameters in single molecules. We show the stiffness and dissipation as measured in the titin molecules along with the noise analysis and calibration methods used.

Chapter 2

Theory

This chapter gives details about a few concepts which will help us understand the experimental methods used here. I will first discuss the technique of Single Molecule Force Spectroscopy. Then I will look into the mechanical models describing the dynamics of cantilever which will help us analyze the data from the force spectroscopy experiments. And finally, I will move on to discuss the viscoelastic properties of Single Molecules, in this case, proteins.

2.1 Atomic Force Microscopy

As the name suggests, Atomic Force Microscopy is the technique of Scanning Probe Microscopy, which uses the information of the force experienced by a sharp tip to image a surface. This is analogous to a blind person reading Braille by feeling the embossed characters while moving his fingers over them. The major advantage of AFM is that it can image surfaces with a sub-nanometer resolution, roughly 1000 times better than optical diffraction limit.

Atomic Force Microscope (AFM) works by measuring the force between a probe and a sample. Figure 2.1 shows the basic components of AFM. The probe is a sharp tip (radius 1-10 nm) attached to a cantilever beam of few hundred micron length and width. Using the precise control of piezoelectric elements, the sample is scanned with respect to the tip. The topographic features on the sample surface proportionally change the force acting on the

cantilever causing it to deflect vertically. Thus by looking at the deflection of the cantilever, one can reconstruct the topography of the surface.

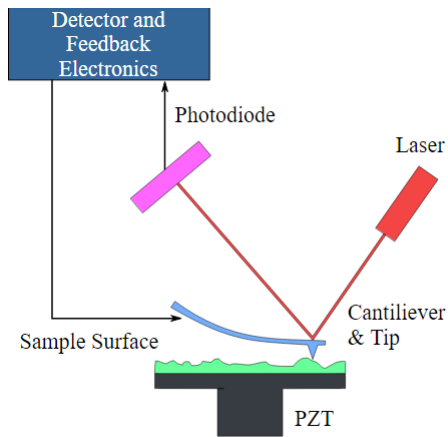


Figure 2.1: Schematic showing basic components of an Atomic Force Microscope (www.wikipedia.com/AFM)

The schematic shows the primary components of an AFM which are, the sample stage assembly, the cantilever holder, the detector assembly, and the feedback electronics. The sample stage consists of the sample mount and piezoelectric assembly responsible for the motion of the sample in X, Y, and Z direction. The cantilever holder is where the cantilever is fixed typically using an S-shaped spring it also consists of the laser which is incident on the back side of the cantilever and an alignment mechanism to help adjust the laser spot. The detector assembly primarily consists of a quadrant photodetector on which the laser spot reflected from the cantilever is incident using adjustable mirrors. The feedback is a Proportional Integral and Derivative (PID) control mechanism, which helps in keeping constant deflection while imaging.

2.1.1 Force Spectroscopy

The AFM can also be used to measure the mechanical force between the sample and the cantilever tip. It is used to measure the force required to rupture a bond which in principle, can be used for chemical identification of atoms and thus termed as force spectroscopy. The technique of measuring this force as a function of the separation between the tip and sample is called force spectroscopy. The cantilever is approached towards the sample until a

certain set-point deflection is reached and then retracted back with constant velocity for a specified distance. According to Hooke's law, the deflection in the cantilever is proportional to the force experienced by it, the constant of proportionality being the stiffness. Thus, by measuring the deflection of the cantilever of known stiffness, we can determine the force exerted on the cantilever by the sample. The tip radius of the AFM cantilever is around 2-5 nm which, is comparable to the size of biomolecules. We can sparsely decorate the surface with very dilute concentration of protein. This allows picking single molecules with AFM tip at a time. Thus, we can essentially perform force spectroscopy experiments on individual single molecules. Figure 2.2 shows the general scheme of force spectroscopy of protein molecules using AFM. The topmost (i) is a schematic of the experimental setup. (ii) depicts the unfolding process and shows how the protein construct undergoes one-by-one domain unfolding. (iii) shows the respective force versus extension plot again indicating the one-by-one unfolding process represented by the saw-tooth pattern in the force measured while pulling the protein.

2.1.2 Dynamic Force Spectroscopy

Conventionally, force spectroscopy involves measuring a steady cantilever deflection signal and determining the force using Hooke's law. This allows the measurement of force required to unfold a protein but, it is difficult to interpret the nature of this force. It gives no information about the dynamic response of the sample like the stiffness and dissipation, which is the elastic and loss modulus respectively. This viscoelastic response can be measured by modulating the cantilever in sinusoidal fashion and measuring the amplitude and phase response of the cantilever, which can be related to the elasticity and dissipation by modeling the cantilever as forced damped harmonic oscillator.

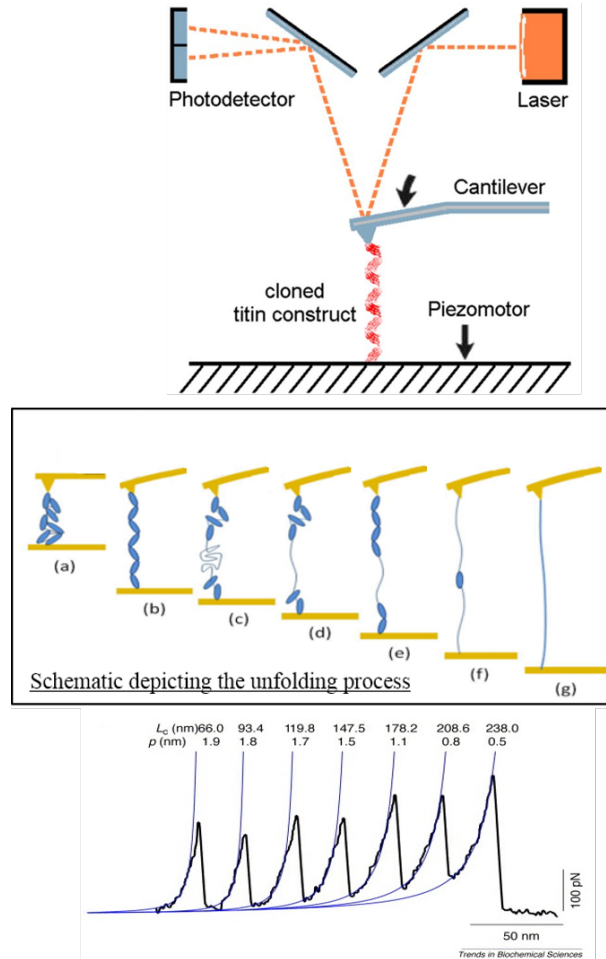


Figure 2.2: **Method of Force Spectroscopy using AFM;** (i) Shows a typical protein pulling experiment using AFM. (ii) shows the depiction of the unfolding process of the poly-protein construct. Note how the domains unfold one after another with increasing extension., (iii) plot shows a typical force versus extension plot observed during the protein unfolding. Each individual peak corresponds to a domain being unfolded under external force. The saw-tooth pattern is related to the behaviour of a protein to the worm-like-chain model in polymer physics.

2.2 Oscillator Models for Cantilever

In order to determine the linear viscoelastic response of the sample, we use simple harmonic oscillator models of the cantilever. In this subsection I will discuss two types of models; the conventional point mass model and the continuous beam model.

2.2.1 The Point-Mass Model

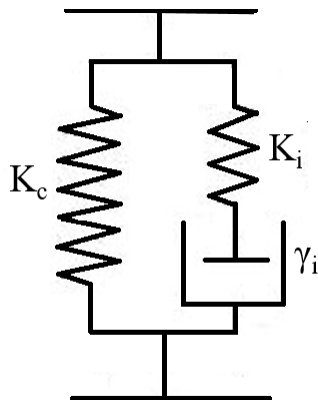


Figure 2.3: Point mass model representation

As the name suggests, this model assumes the cantilever to be a point object attached to a massless spring of stiffness k_c . The sample in our case, a single protein molecule, is modeled as a spring which shows up as interaction stiffness k_i and a dash-pot which causes damping of the cantilever motion and is quantified by the friction term as γ_i

The equation of motion for such a system is given by the standard equation for forced damped harmonic oscillator:

$$m^* \frac{d^2 z}{dt^2} + \gamma \frac{dz}{dt} + k_c z = A_0 e^{i\omega t} + k_i z \quad (2.1)$$

Where m^* is the effective point-mass, γ is the combined dissipation due to dissipation in the sample and the hydrodynamic damping of the cantilever, $\gamma = \gamma_i + \gamma_c$. A_0 is the free amplitude of the cantilever, ω is the drive frequency. This is a standard equation and the has standard solutions for Amplitude and phase as

$$\text{Amplitude : } A = \frac{k_c A_0}{\sqrt{(k_c + k_i)^2 \left(1 - \frac{\omega^2}{\omega_o^2}\right) + (\gamma_i \omega)^2}} \quad (2.2)$$

$$\text{Phase : } \phi = -\tan^{-1}\left(\frac{\omega \gamma_i}{(k_c + k_i) \left(1 - \frac{\omega^2}{\omega_o^2}\right)}\right) \quad (2.3)$$

Now, in off-resonance limit, i.e. when ω is much less than the resonance frequency ω_o , these solutions can be used to derive the expressions for the stiffness k_i , and the dissipation γ_i due to the sample molecule in terms of the amplitude and phase of the cantilever which can be measured experimentally using Lock-in amplifier. The stiffness is given by:

$$k_i = k_c \left(\frac{A}{A_0} \cos\theta - 1 \right) \quad (2.4)$$

and dissipation is given by

$$\gamma_i = -k_c \frac{A_0}{A \omega} \sin\theta \quad (2.5)$$

The point-mass model of the cantilever is very successful in determining the atomic dissipation in Ultra-High Vacuum(UHV) conditions. It also works well for while measuring nano-scale dissipation in ambient conditions owing to the negligible drag force which air exerts on the cantilever as opposed to liquid environment.

2.2.2 The Continuous Beam Model

A recent publication from Benedetti et.al. (September 2016)[19] claimed that there exists a fundamental problem with the adequacy of simple one-dimensional damped harmonic oscillator model to measure the viscoelastic properties of single molecules for the following reasons. (a.) The cantilever is not a point-mass and has its own frequency-dependent response for external mechanical drive which can be derived from beam theory. (b.) The approximation of point-mass ignores all the damping experienced by the cantilever which is expected to be much greater than the dissipation in single molecules. This gives us bizarre values of dissipation.

Benedetti et.al. provided a solution for the above problem and state that dynamics of the cantilever can be described correctly by a 4th order Partial Differential Equation. The proposed model of the cantilever is of a a Forced dithering motion of a solid continuous beam inside a viscous liquid. The equation of the free end of the cantilever is thus given by,

$$-\tilde{\rho}\tilde{S}\frac{\partial^2 z}{\partial t^2} - \gamma_c\frac{\partial z}{\partial t} = EI\frac{\partial^4 z}{\partial x^4} \quad (2.6)$$

Where $\tilde{\rho}\tilde{S} = \rho S + m_a$: ρ is the mass density, S is the cross section area and m_a is the effective hydrodynamic mass of the cantilever beam. γ_c is the viscous damping coefficient of the cantilever, E is the Young's modulus of the material and I is the moment of inertia of the beam which is $\frac{bh^3}{12}$. The solution to this 4th order PDE 2.6 is obtained by using 4 boundary conditions and the solutions are obtained in the form of amplitude and phase which are given by,

$$R \cong \frac{A}{2k_c L} \sqrt{(3k_i - \tilde{\rho}\tilde{S}\omega^2 L)^2 + \omega^2(3\tilde{\gamma}_i + \gamma_c L)^2} \quad (2.7)$$

and

$$\theta \cong \tan^{-1}\left(\omega \frac{3\tilde{\gamma}_i + \gamma_c L}{3k_i - \tilde{\rho}\tilde{S}\omega^2 L}\right) \quad (2.8)$$

Since we know that, $R = \sqrt{X^2 + Y^2}$ and $\theta = \tan^{-1}(\frac{Y}{X})$ It is apparent from equations 2.7 and 2.8 that they can be separated into X and Y components as

$$X = \frac{A}{2k_c L}(-3k_i + \tilde{\rho}\tilde{S}L\omega^2) \quad (2.9)$$

$$Y = \frac{A\omega}{2k_c L}(3\bar{\gamma}_i + \gamma_c L) \quad (2.10)$$

By simply rearranging the terms in equations 2.9 and 2.10, we can determine the stiffness and dissipation in single molecules as follows,

$$k_i = \frac{1}{3}(\tilde{\rho}\tilde{S}L\omega^2) - \frac{2}{3}\left(\frac{k_c L X}{A_0}\right) \quad (2.11)$$

and

$$\bar{\gamma}_i = \frac{3k_c L Y}{3A_0 \omega} - \frac{\gamma_c L}{3} \quad (2.12)$$

We can see in equation 2.11, the stiffness k_i is represented by two terms, the first one is the elastic contribution arising from the cantilever and depends on its material and geometry and is constant. The second term is the stiffness arising due to the change in X signal with respect to the free amplitude of the cantilever and the cantilever stiffness. Similarly, the dissipation 2.12 consists of two terms, first term corresponds to the dissipation from indicated by the changes in Y signal. The second term is the constant hydrodynamic drag experienced by the cantilever due to the surrounding liquid.

Thus the method proposed by Benedetti et.al. [19] shows that, for a cantilever oscillating in liquid, the X component of the Lock-in amplitude is dependent on the stiffness and Y-component is dependent on dissipation alone. This allows a direct and independent measurement of these quantities simply by measuring the X and Y component of the Lock-in amplitude which is nothing but the output of the two phase sensitive detectors of the Lock-in amplifier.

Chapter 3

Methods

This chapter covers the experiential details about the instrument used for the experiments this project and the procedure of experimentation.

3.1 The Instrument

This project is based on a home made instrument called Small Amplitude AFM. This is an Atomic Force Microscope specifically designed for force spectroscopy application. The remarkable feature of this instrument is that it uses a fiber optic based interferometer to detect the cantilever deflection unlike commercial AFMs which use a quadrant photodiode. The interferometer is a Fabry-Perot type and can potentially have sensitivity 300 times the conventional detection systems. The schematic 3.1 shows the components of the setup which are discussed in the following subsections.

1. Interferometer assembly.
2. Sample stage assembly.
3. Control Electronics and LabVIEW interfacing.

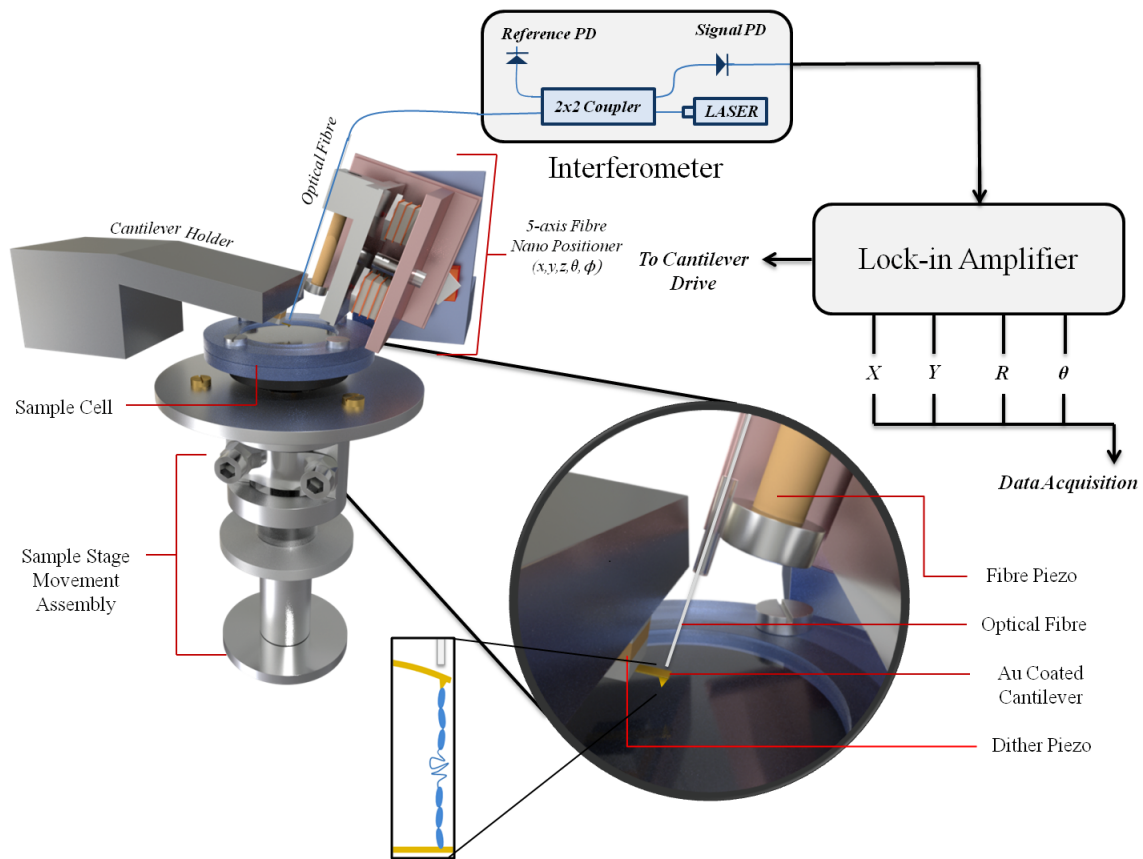


Figure 3.1: Schematic of the Home-built Small Amplitude Atomic Force Microscope

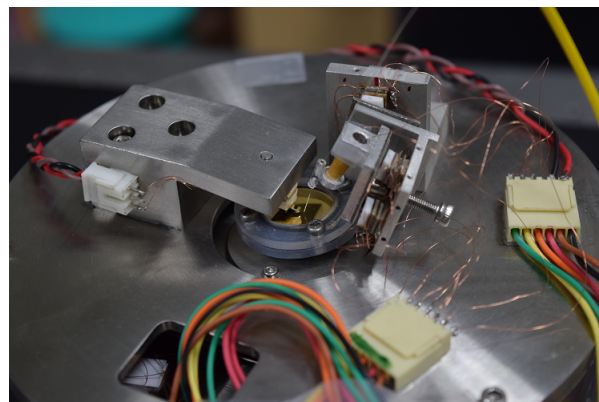


Figure 3.2: Photograph of the Small Amplitude Atomic Force Microscope

3.1.1 Interferometer Assembly

The Interferometer assembly consists of the optic fiber, the fiber positioner, the Laser diode and a 2X2 coupler. The logic is to align the end of the fiber perfectly parallel to the back of the cantilever which acts as a Fabry-Perot etalon. This interferometer configuration produces extremely sharp fringe pattern which directly results in higher sensitivity of deflection detection. The process is discussed in detail below.

Fiber Preparation: The end of the fiber needs to be perfectly flat and partially reflective for the etalon to form. The fiber is hence cleaved with a high precision cleaver which makes the end of the fiber perfectly flat. The reflectivity after cleaving is just 0.4-0.5%. To increase the reflectivity, the fiber is dipped into a metal-organic precursor (Titanium-(IV)-ethylhexoxide) dissolved in xylene (1:2 by weight) and flashed into the blue flame of a Butane torch. This burns away the organic compound and deposits a uniform thin layer of TiO_2 at the end of the lever which increases the reflectivity of the end to 15-25 % . The fiber is then mounted in a hollow glass ferrule using *Fevikwik* superglue. This method was first used by Hoffmann et.al [20]

Fiber Nano-Positioner: The fiber is mounted on a nano-positioner which helps in aligning the fiber perfectly perpendicular to the cantilever so that its reflective end is parallel to the cantilever. The ferrule which holds the fiber is mounted on a tube piezo which can expand or contract along the normal z-direction. This piezo is then mounted on a assembly consisting of two mutually perpendicular slider plates held by screw magnets. Each of these plates have 3 stacks of shear piezos that are arranged in a fashion such that by giving certain logic pulses they are capable of producing motion in $XZ\theta$ and $YZ\phi$ directions respectively. The mechanism of movement is the stick slip motion due to the slowly rising and rapidly falling voltage pulses given to the piezos. Thus we have a five-axis positioner which can move the fiber in X, Y, Z, θ and ϕ directions.

The Interferometer: The light source is an infra-red diode LASER of wavelength 1310 nm and power 1 mW. The LASER output first goes into the 2X2 coupler where it is split into two optical fibers; half of the light falls on a reference photodiode and the other half goes to the coated fiber end. Light is reflected back from the partially reflective end and also

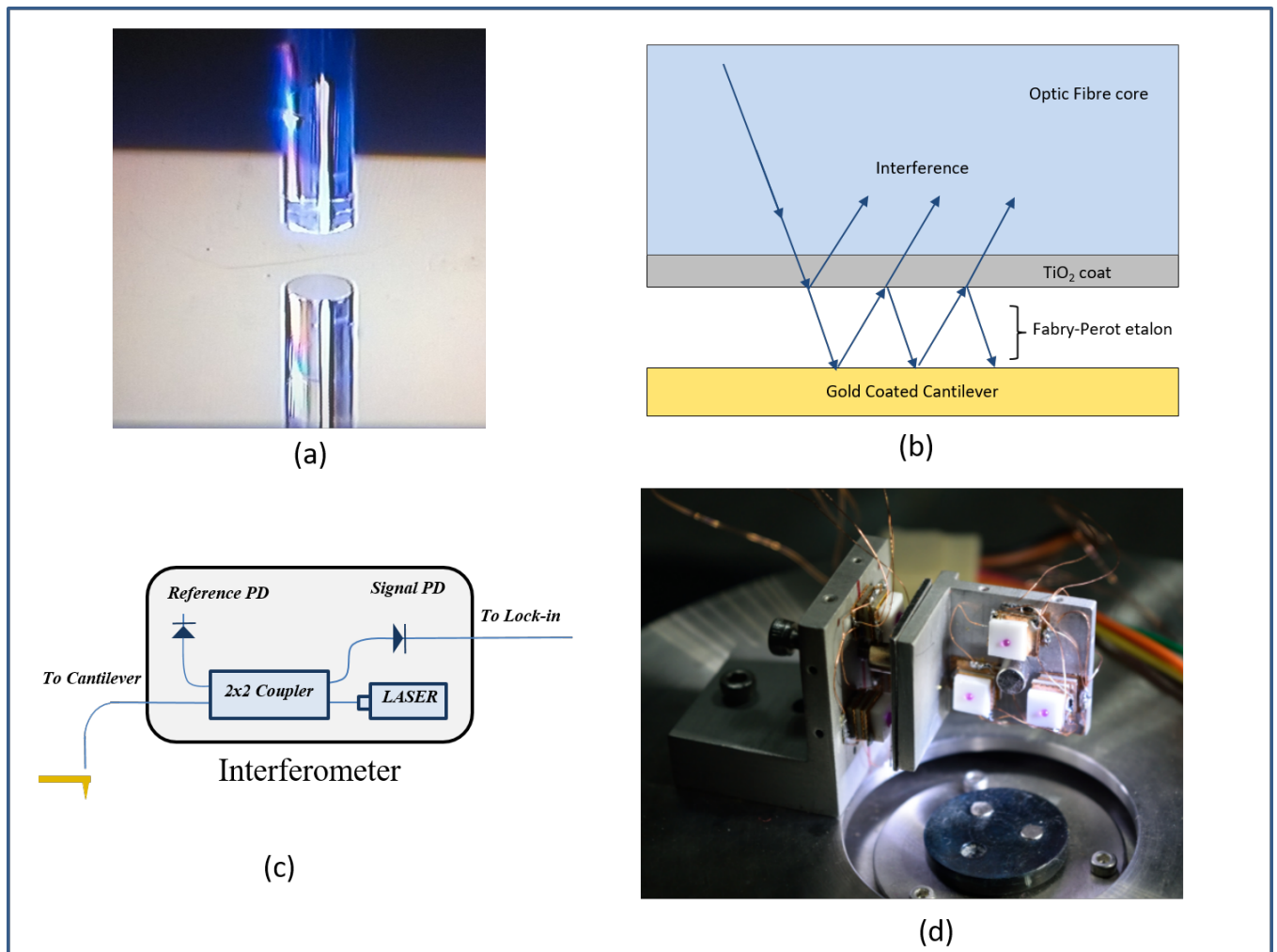


Figure 3.3: **The Fiber Interferometer assembly** (a) is a photograph showing the end of the TiO_2 coated fiber and its reflection from the base of the cantilever. The reflection shows the flatness of the fiber end. (b) is a schematic depicting the formation of the Fabry-Perot etalon between the Fiber end and the back of the cantilever. (c) is a schematic showing the mechanism of interferometric detection. (d) is a photograph of the penta-axis Fiber slider mechanism. We can see the two plates, having 3 piezo stacks and a screw magnet in the center.

from the back of the cantilever which results into an interference pattern. This light again goes to the 2X2 coupler where half of the light goes on the signal photodiode and the other half goes back into the laser. The intensity of laser incident on the signal and the reference photodiode is compared to give a equivalent voltage output.

The interference pattern incident on the signal photodiode is a function of the distance between the two mirrors (the fiber end and the cantilever). The interference pattern is recorded by varying the distance which is achieved by changing the voltage to the tube piezo. The algorithm then plots this function and finds the voltage value to the piezo where the slope of the interference pattern is highest. The slope of the interferometer indicates the amount of voltage signal generated from the photodiode due to given displacement of the fiber. Figure 3.4 shows an instance of alignment where the slope is observed to be around $273 \text{ mV}/\text{\AA}$ meaning, that every angstrom displacement of the gives the photodiode output voltage to be 273 mV. Once the alignment is complete, the PI feedback is activated with the setpoint as the maximum slope and thus locks the fiber in quadrature. This feedback gives a correction voltage once every 200 milliseconds which is sufficient to correct slow drifts caused in the instrument. We oscillate the cantilever with frequency of 2 KHz which faster than what the feedback can correct for thus, the fast oscillations of the cantilever are bypassed through the feedback and we can measure their amplitude using Lock-in amplifier.

This describes the construction and the working of the Fiber Interferometer assembly. The software used to control the interferometer is SPM(version 1.16.13.7) from NanoMagnetics Instruments.

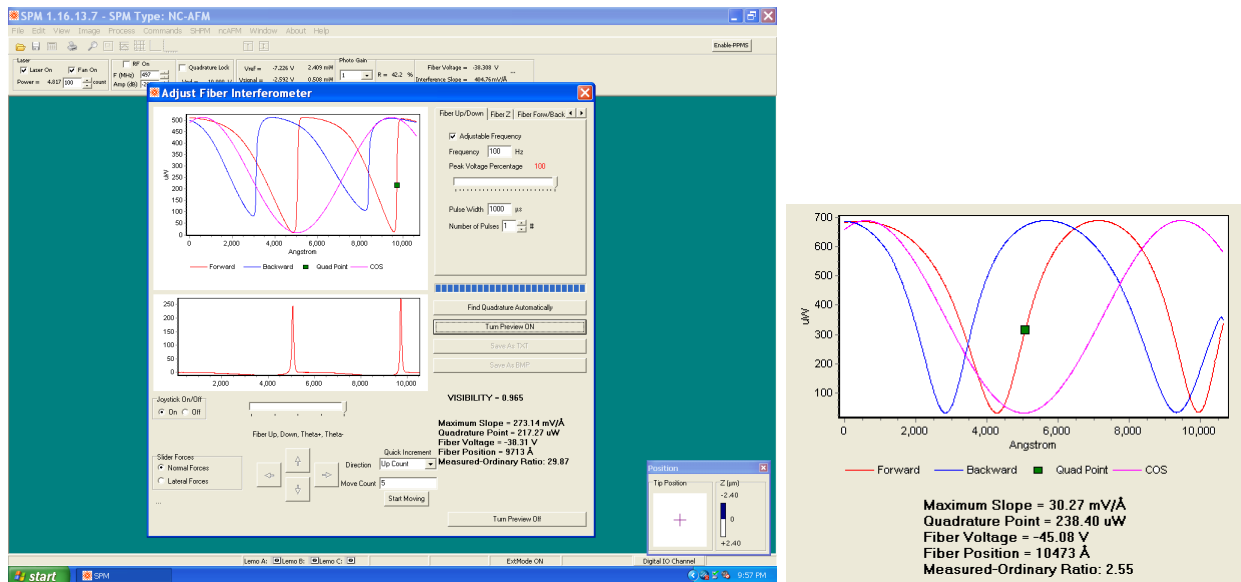


Figure 3.4: The SPM software used to align and lock the fiber in quadrature. The fiber is locked at the slope of $273.14 \text{ mV}/\text{Å}$. However, This slope is too high for the feedback to lock on due to limited resolution of the DAQ card because of which the feedback keeps jumping between two values. To avoid this during experiments, we use a slightly imperfect cavity aligned at slopes $30\text{-}50 \text{ mV}/\text{Å}$. The inset shows interference pattern of maximum slope of $30.17 \text{ mV}/\text{Å}$.

3.1.2 Sample Stage assembly

The sample stage consists of two piezo actuators: the Hammer piezo and the Scanner piezo. The objective of this assembly is to move the sample in X Y and Z directions. The hammer piezo is used for coarse motion in the normal Z direction. It consists of a cylindrical piezo with a steel weight attached at the bottom, and a glass tube attached at the top. The assembly is held in place by a leaf spring which presses against the glass tube. The motion of the hammer is based on the inertial sliding principle (also called as stick-slip motion). The piezo is subjected to a high voltage pulse which slowly rises and sharply falls after a specified value. During the slow rise, the cylindrical piezo steadily contracts proportionally to the voltage applied. Now, as the pulse falls sharply, the hammer tends to expand almost instantly but, the inertia of the steel plate prevents it from sudden motion. The hammer can expand only in one direction which is vertically upward. This motion results into a higher force than the frictional force due to the leaf spring pressing against the glass tube and this results into the stick slip motion. While retracting, a pulse of opposite polarity is given which expands the hammer piezo causing the hammer to move down. When the voltage suddenly drops to zero, the assembly is pulled downward again owing to high inertia of the hammer. The extent of motion in one pulse of around 100 V to the hammer piezo is roughly $50 \mu\text{m}$.

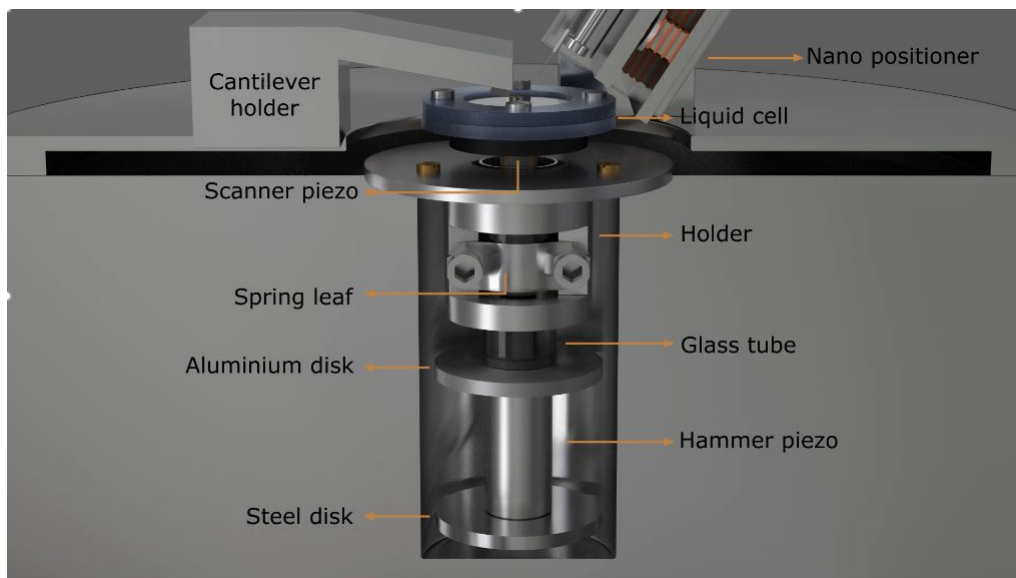


Figure 3.5: A schematic showing the components of the sample stage assembly

The scanner tube piezo is placed inside the glass tube. It has a electrically continuous inner wall but, the outer wall is split into 4 faces equally. By applying equal voltages to all the faces, one can cause fine movement in normal Z direction. Giving opposite voltages to opposite faces causes one face to shrink while causing other to expand thus causing a resultant bending by a small angle. This can be considered as a lateral motion since the curvature is little as compared to the height of the piezo. Thus we can achieve fine motion in X, Y and Z direction. Typically, applying 50 V and -50 V to the opposite scanner faces causes $5\mu\text{m}$ displacement in X or Y direction. The fine Z motion known to be 21 nm/V and was calibrated using interferometer. The scanner piezo has a magnetic stage attached on the top which hold the liquid cell.

3.1.3 Control Electronics and LabVIEW interfacing

To hold the cantilever at fixed separation from the surface before every experiment, we need a feedback control mechanism. We observe that the amplitude decreases to 10% of the free amplitude upon approach. This variation takes place within the distance of 2-3 nm from the surface in a linear fashion. Hence, we use the amplitude signal to hold the tip-surface separation fixed.

The electronic components of the setup are the PI feedback mechanism and the sample stage controller.

The PI feedback is a simply Proportional and Integrator based feedback mechanism which takes input, compares it to a given set-point and gives the output so as to bring the input equal to the set-point. The set-point in our case is the cantilever oscillation amplitude. It is observed that the cantilever amplitude drops significantly as we approach it towards the surface. We define the contact as the point where the cantilever amplitude drops to half its value when it is free. We can use the feedback to hold the cantilever in contact by monitoring its amplitude.

The sample stage controller is a circuit which takes in the voltage values to be given in the X, Y or Z direction, translates it into the voltages to be given to the scanner piezo(Z+X, Z-X, Z+Y, Z-Y) using OpAmp (CA 3140) based adder and subtracter, amplifies it using high voltage amplifiers(PA 88). The voltage output from the DAQ card has the range ± 10

Volts however, to produce significant movement (in a few μm) we need voltages as high as 150 V which is exactly the purpose of using high voltage amplifiers.

The following part discusses the procedure of the force spectroscopy experiments. It is better explained using the flow charts as shown in Figures 3.6, 3.7, 3.9. The programming of these instrument control procedures are done in NI LabVIEW(2011) software and were developed by Ajith V.J. in our lab. The data acquisition and control signalling is done using 16-Bit DAQ card (NI USB-6363) from National Instruments. The major steps involved are better described using the flowcharts as shown below.

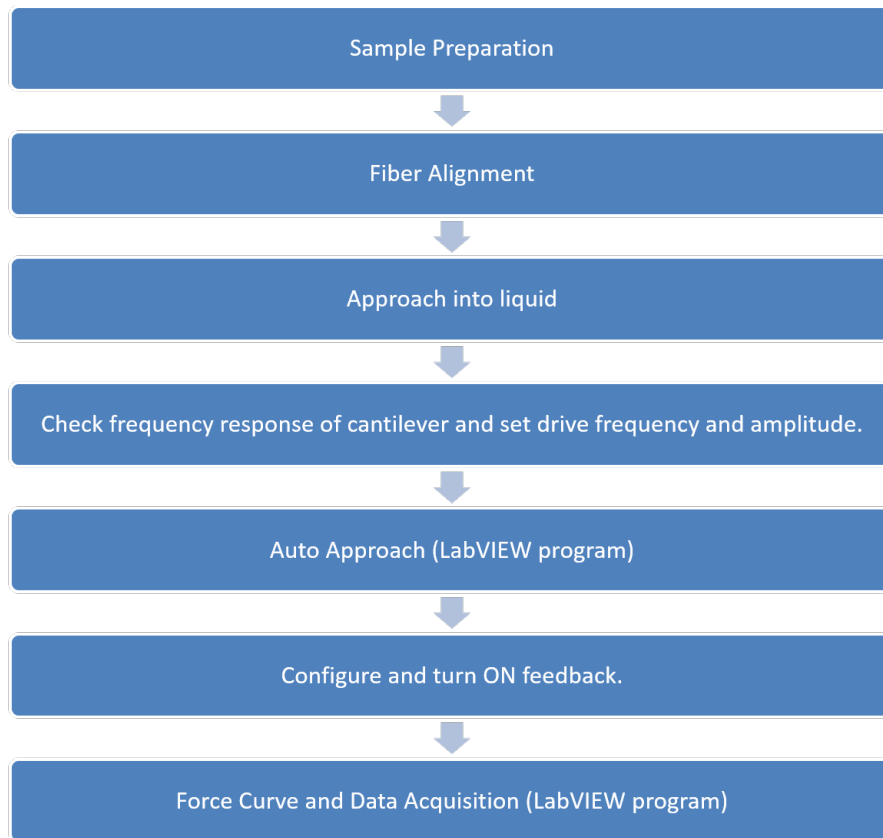


Figure 3.6: Flow chart illustrating the complete experimental procedure

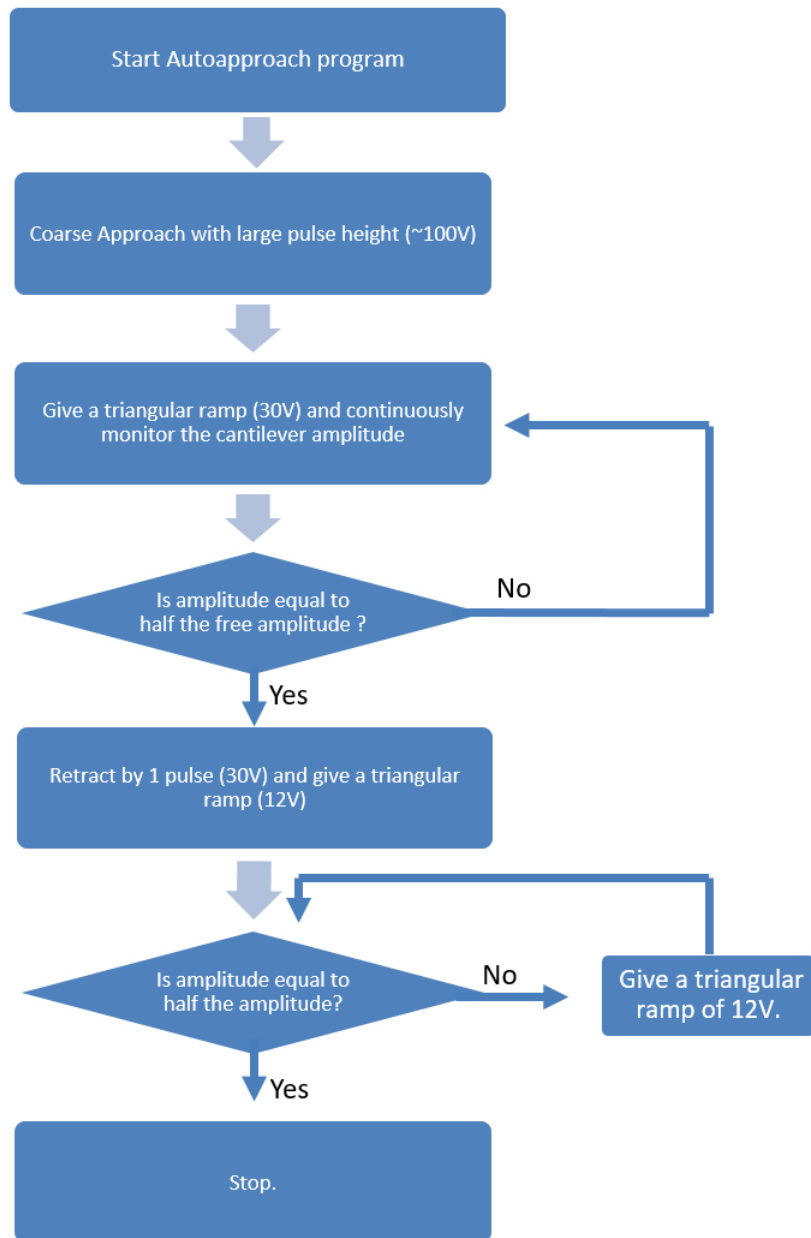


Figure 3.7: Flow chart illustrating auto-approach algorithm implemented in LabVIEW program

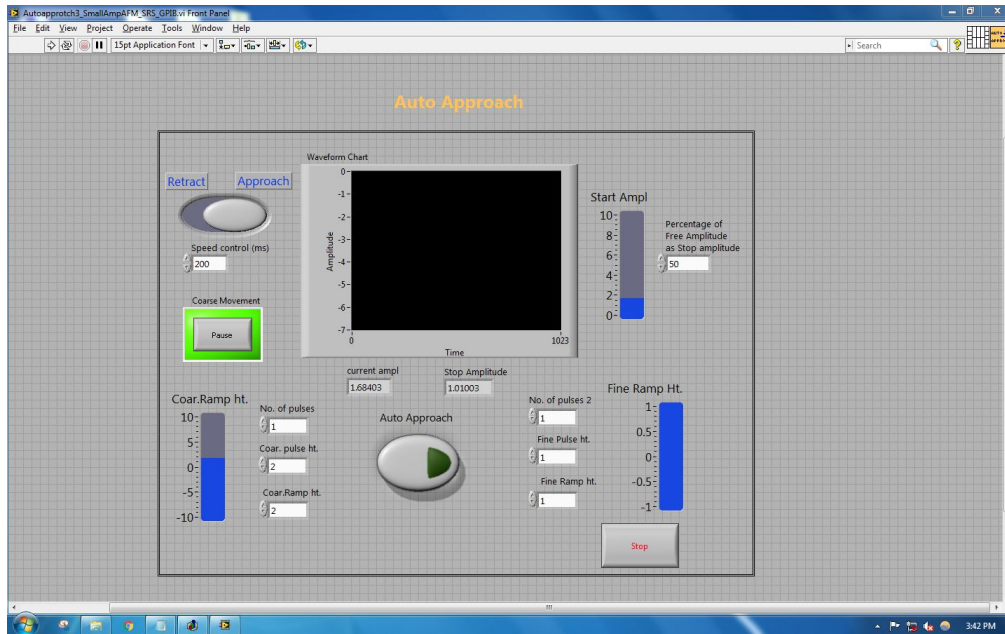


Figure 3.8: The front panel of the Auto-approach program in NI LabVIEW 2011 software

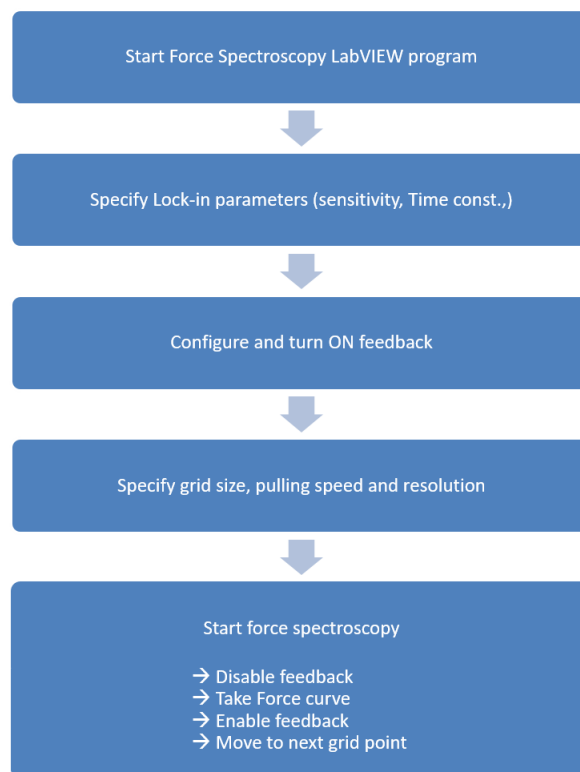


Figure 3.9: Flow chart illustrating the procedure of operating the Force Spectroscopy and Data Acquisition program in LabVIEW.

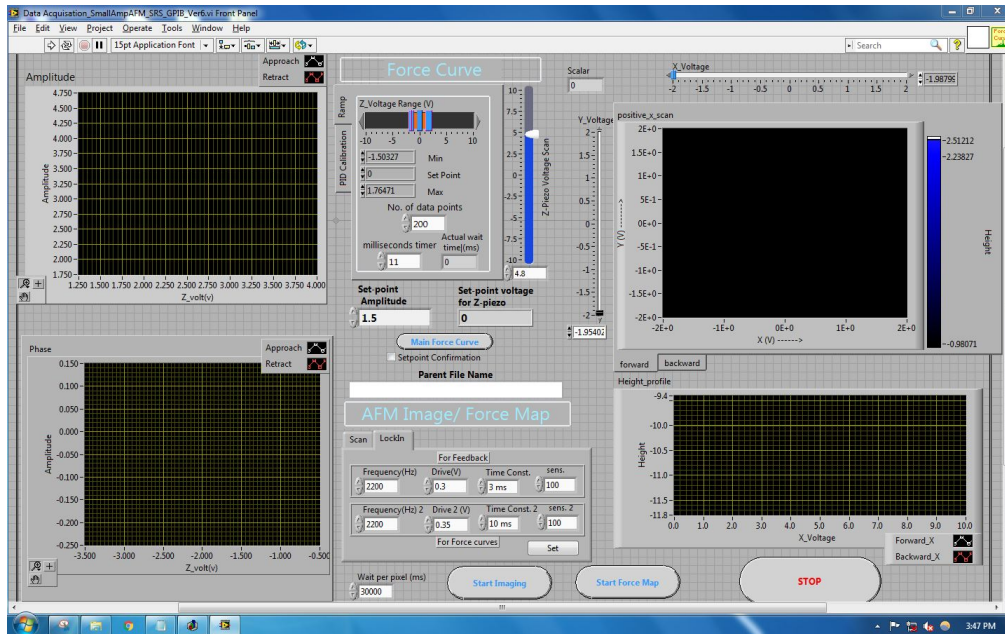


Figure 3.10: The front panel of the force spectroscopy and data acquisition program in LabVIEW 2011 software.

3.1.4 Calibrations

The instrument is interfaced with the computer and is controlled using voltage signals given to the piezos. In order to know what voltage corresponds to what displacement in the piezo, we need to calibrate the piezos.

3 important calibrations are required in this setup.

1. Fiber piezo calibration
2. Scanner Z calibration
3. Scanner X-Y calibration

Fiber Piezo calibration: The fiber piezo is responsible for the movement of fiber while recording the interference pattern and maintaining it into the feedback. It needs to be calibrated by specifying a k_{Fiber} parameter in the SPM software settings which represents the displacement of the fiber per unit applied voltage. The calibration method is as follows.

1. Align the fiber perpendicular to a reflective surface such that some interference pattern is recorded due to the forward-backward movement of the fiber piezo by giving a known voltage. (need not be the best alignment)
2. The interference pattern is nothing but the Airy function corresponding to the Fabry-Perot etalon. We know that adjacent peaks in the airy function are separated by distance equal to half the value of the wavelength of light used.
3. The light source used is a Laser diode with wavelength 1310 nm. Thus the distance between two Airy functions should be 655 nm. Now, since we know the distance, we can adjust the value of k_{fiber} in $\text{\AA}/\text{mV}$ by looking at the interference pattern output till it shows the correct distance between two peaks.
4. The k_{fiber} value depends on the dimensions and sensitivity of the fiber piezo and hence needs to be changed whenever the piezo or the soldering is changed. For current configuration, the k_{fiber} constant is calibrated at $128 \text{\AA}/\text{mV}$.

Scanner Z calibration: The scanner piezo movement in Z direction needs to be calibrated accurately because parameters such as extension and pulling speed directly depend on this value. This is achieved using following steps.

1. Align the fiber perpendicular to a reflective surface (gold coated coverslip) placed on the sample stage such that some interference pattern is recorded due to the forward-backward movement of the fiber piezo.
2. Disable the fiber piezo movement by removing the voltage supply. The interference pattern on the screen will now change to a constant intensity value.
3. Give a known amount of voltage to the scanner to cause movement in Z direction (all faces are given the same voltage). Record the constant value of intensity falling on the photodiode for every voltage provided.
4. Plot the recorded intensity versus the applied voltage. This should recreate the interference pattern however, its the scanner piezo that moves in this method.
5. Similar to the above method, we can find the calibration in the form of the displacement per applied voltage in nm/V . In our setup, we found this value to be $21.43 \text{ nm}/\text{V}$

X-Y scanner calibration: X-Y scanner calibration is important to know the extent of horizontal displacement while taking a grid of force curves. For X-Y calibration, the AFM is used in the imaging mode. We used a tuning as a force sensor to image the surface of a DVD. The tracks of the DVD are made of grooves of two sizes representing 0 (length = $0.83 \mu\text{m}$) and 1 (length = $1.66 \mu\text{m}$). The distances between these tracks and dimensions of the grooves is $1.6 \mu\text{m}$ and these distances standardized worldwide. Since we use a sample with groves of known dimensions, we can calibrate the X-Y scanner by from the topography image. Figure 3.11 shows one of the image taken with our instrument and the topography across corresponding to the trace drawn on the image. The distance between two tracks (seen to be as the troughs in the topography trace) is $1.6 \mu\text{m}$, and we know the voltage applied to the piezo while imaging, we found out that the X-Y scanner moves $0.11 \mu\text{m}/\text{V}$ in the horizontal direction.

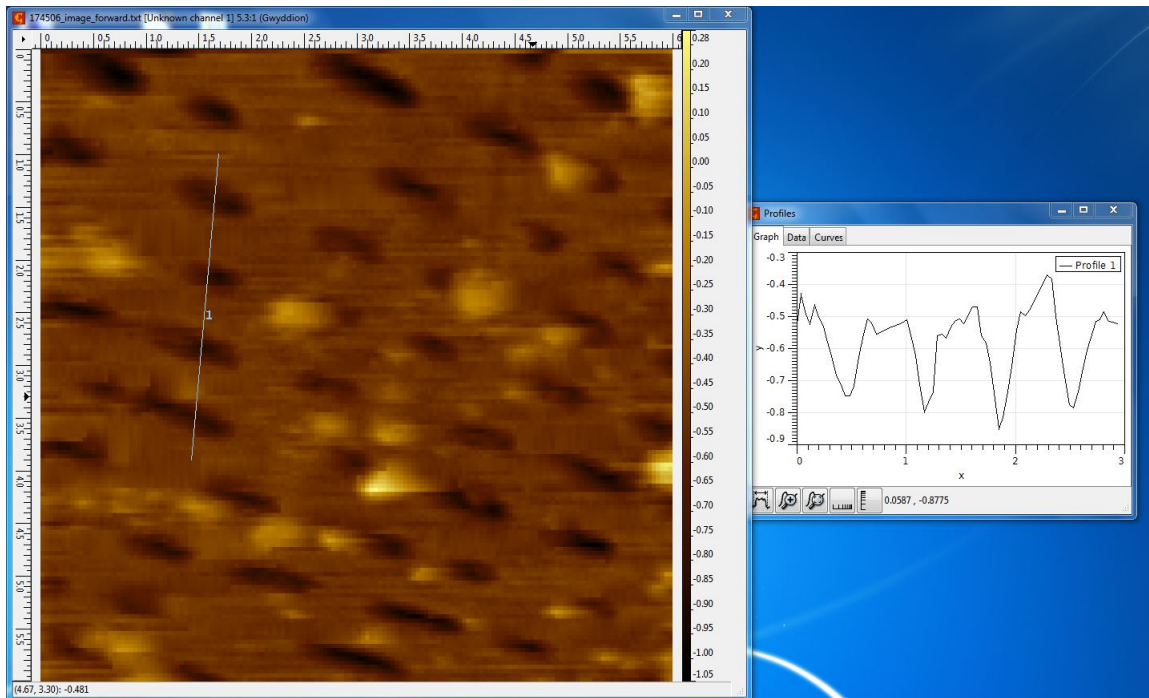


Figure 3.11: X-Y scanner calibration

3.2 Experimental

In this section i will discuss the protocols for sample preparation, and other details for the force spectroscopy experiments on titin I-27 protein molecules.

3.2.1 Sample Preparation Protocol

titin I-27 polyprotein constructs containing seven identical domains in tandem were constructed from a plasmid similar to described in [21]. The plasmid was amplified using PCR and purified using standard liquid chromatography procedure.

PBS buffer at pH 7.4 was used as the standard buffer for all experiments. The protein sample (100 μL) in PBS with a concentration of 10 mg/mL was adsorbed onto a freshly evaporated gold coated coverslip assembled in the liquid cell by incubating it on the substrate for 15 minutes at room temperature. The sample solution was washed three times with PBS to remove the excess un-adsorbed protein from the working solution. After the wash, the liquid cell was again filled with PBS which acts as the liquid medium for further experiments. In order to prevent biological contamination, the gold coverslips were ozone treated for 30 minutes prior to sample preparation.

After completion of sample preparation, the fiber is aligned at the back of the cantilever and the assembly is submerged into the PBS buffer by moving the stage assembly upwards. Using the amplitude signal for feedback control, the surface is auto-approached towards the tip. The point of approach was defined to be the tip-sample separation where the amplitude of the cantilever reduced to 50% of the free amplitude during approach. The actuation and data acquisition is performed using a LabVIEW program as discussed in section 3.1.3.

3.2.2 Force Spectroscopy Experiment

After the auto-approach, we start the force spectroscopy program based on LabVIEW. We specify the drive frequency and amplitude, Lock-in sensitivity, pulling velocity, etc. The next step is to set the feedback ON. This involves specifying the set-point amplitude and determining the necessary voltage to be given to the z piezo to attain that set-point. Finally, the area for the grid and its resolution is specified which is typically $6\mu\text{m} \times 6\mu\text{m}$ area and covers 64 to 100 measurements in one run.

Commercially available micro-fabricated cantilevers from μ masch (HQ:CSC37/Cr-Au) are used for the experiments throughout the study. These cantilevers have a gold coating of 50 nm on their backside with a chromium coating of 30nm under it to strengthen the gold coat. This coating helps in increasing the reflectivity of the backside of the cantilever which in turn helps us to form a high finesse interferometer cavity. The cantilevers have the dimensions of length = $250 \pm 5\mu\text{m}$, width = $35 \pm 3\mu\text{m}$ and thickness = $2 \pm 0.5\mu\text{m}$. The stiffness of these cantilevers is calibrated using commercial AFM (JPK Nano Wizard-II) by thermal noise analysis method. The stiffness values are typically found to be around 0.8 N/m to 1 N/m and the resonance frequency is around 30 kHz in air and 10-12 kHz in water.

The cantilever is oscillated at off resonance frequency of 2-2.2 kHz where the frequency response is flat. The experiments are carried out at drive amplitudes of 0.5-2 Å. During a force curve, the protein terminus binds to the tip of the cantilever by non-specific interactions with a certain probability. After a set waiting time, the sample is retracted with a constant velocity which ranges between 50 nm/s to 400 nm/s. The upper limit is due to the time constant limitation of Lock-in amplifier (lowering the time constant is not a solution as it increases the noise in measurement.) and the lower limit is because lowering the pulling speeds increases the chance of protein to unfold spontaneously thus disrupting our measurement. The stiffness and dissipation are measured at every point during the unfolding of titin I27 polyprotein.

Chapter 4

Results

This chapter describes the important results of this project. The home-built small amplitude AFM setup was used to study mechanical unfolding experiments of titin I27 polyprotein and using the methods discussed in previous chapter.

4.1 Measurement and Data Analysis

We measure X and Y components from Lock-in amplifier and calculate the Amplitude and Phase from $A = \sqrt{X^2 + Y^2}$ and $\tan^{-1}(Y/X)$ respectively. We also record the amplitude and phase outputs from the lock-in amplifier for comparison and find that they are similar with slightly more noise in the direct measurement.

In figure 4.1, we show one of the protein unfolding curves depicting the unfolding signatures of titin I27 protein which is confirmed by the contour length of unfolding domain peaks being standard 25 nm. Benedetti et.al., tried the same experiment using commercial AFM and reported that the y-component of the signal was completely featureless in the region where the protein was being mechanically unfolded. From this non-observation, they established an upper limit on the dissipation in single titin proteins to be 10^{-7} kg/s which, was inferred from the noise floor of the measurement. In the measurements shown in Figure 4.1, we can clearly observe the features in Y-signal corresponding to the unfolding protein. The ability to detect Y-signal in our experiment is attributed to the enhanced deflection detection due to use of the fiber interferometer.

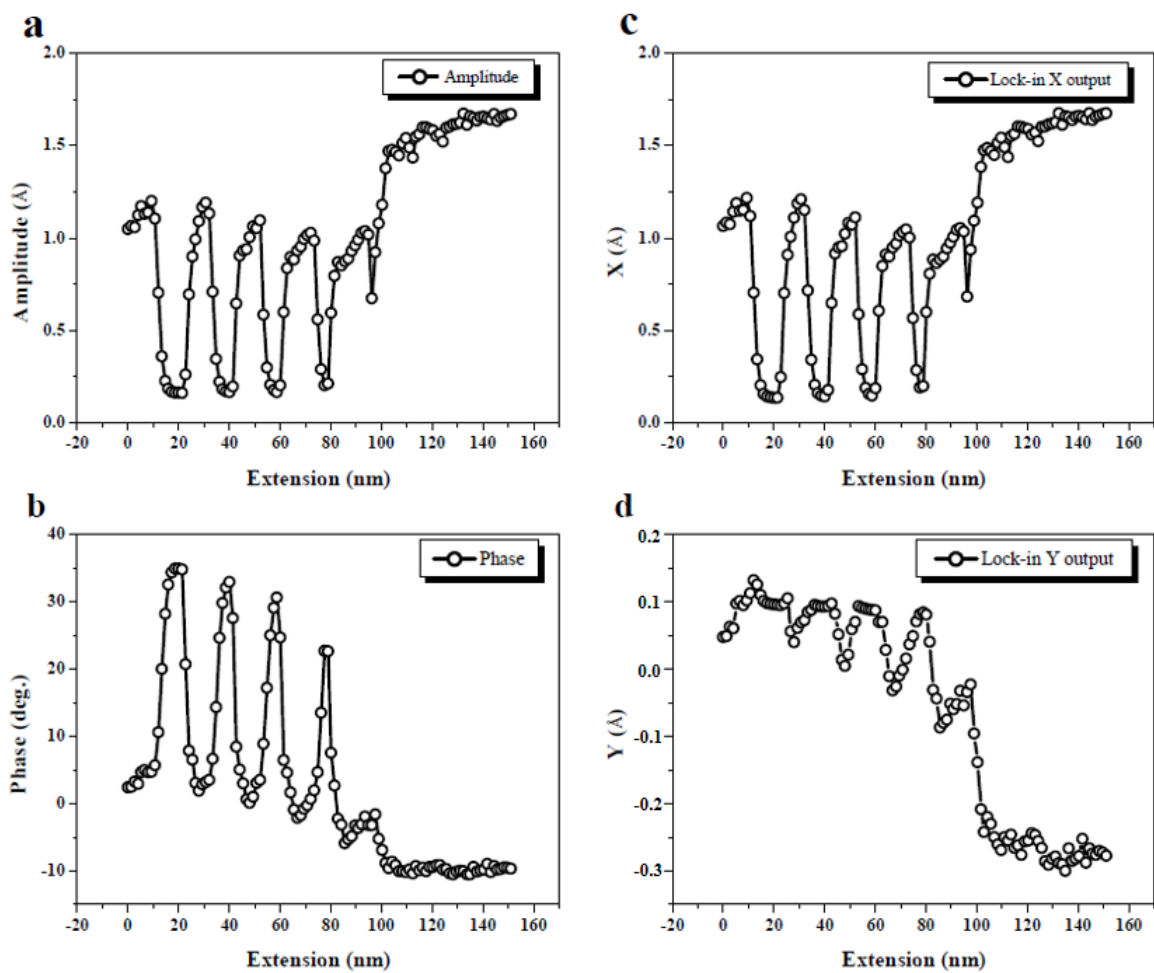


Figure 4.1: Shows the experimental measurements (a)Amplitude of the cantilever, (b)Phase change (c)X component of the amplitude (d)Y component of amplitude. It is observed that the change in Y signal is roughly 10 times smaller than that in X signal.

Comparing amplitude and phase, we see that they roughly follow an inverse relationship i.e. higher amplitude corresponds to lower phase change and vice versa. Comparing X and the Y signal from the unfolding data, we can see that the Y signal is 10 times smaller in feature size than X signal, the extent of variation in X being 1.5\AA and that in Y being 0.1\AA . At certain points (regions where amplitude is minimum 0.1\AA), the magnitudes of X and Y components become roughly equal explaining the unusually high change of 40° in phase.

We will now look at the analysis of the above data to find out stiffness and dissipation using the conventional point-mass model and the newly proposed continuous beam model. The main difference between the two models is that the later does not assume the cantilever to be a point object as opposed to the the former and is quite relevant when we consider the cantilever dynamics in viscous dissipative (liquid) environments. The elegance of the method proposed by Benedetti et.al is that it proves the X and Y signals are related to the stiffness and dissipation independently.

The stiffness and dissipation calculated using the point-mass model are shown in 4.2(a and c) respectively. The point-mass model produces surprisingly large values for stiffness and dissipation. The stiffness lies in the range of 1-4 N/m and dissipation is of the magnitude 10^{-4} kg/s. To put things in perspective, the cantilever stiffness used for this experiment is 0.8-1 N/m. The dissipation observed in the same cantilever, a macroscopic object as compared to a single protein molecule, is of the order of 10^{-6} kg/s. Now, it is highly unlikely that a protein molecule, a biopolymer will be stiffer than a crystalline silicon cantilever. Moreover, it is difficult to imagine how such a small molecule can produce dissipation two magnitudes higher than that of the object which is over a million times larger in size than the protein. Finally, we qualitatively observe the trends of stiffness and dissipation following each other indicating the local Maxwell's relaxation time remains largely unchanged over the unfolding process which suggests that the protein behaves like a Newtonian fluid. This is completely an inconsistent with the role of muscle proteins and their function of handling tremendous stresses.

Parts (b) and (d) in Figure 4.2 show the stiffness and dissipation of the same molecule as calculated using the continuous beam model. The stiffness measured from the X component of amplitude is of the magnitude 10^{-4} N/m, four orders smaller than the previous estimate using point-mass model and is consistent with the single molecule stiffness measured using other techniques [13] [9] [22]. The Dissipation, which is calculated using the Y signal has

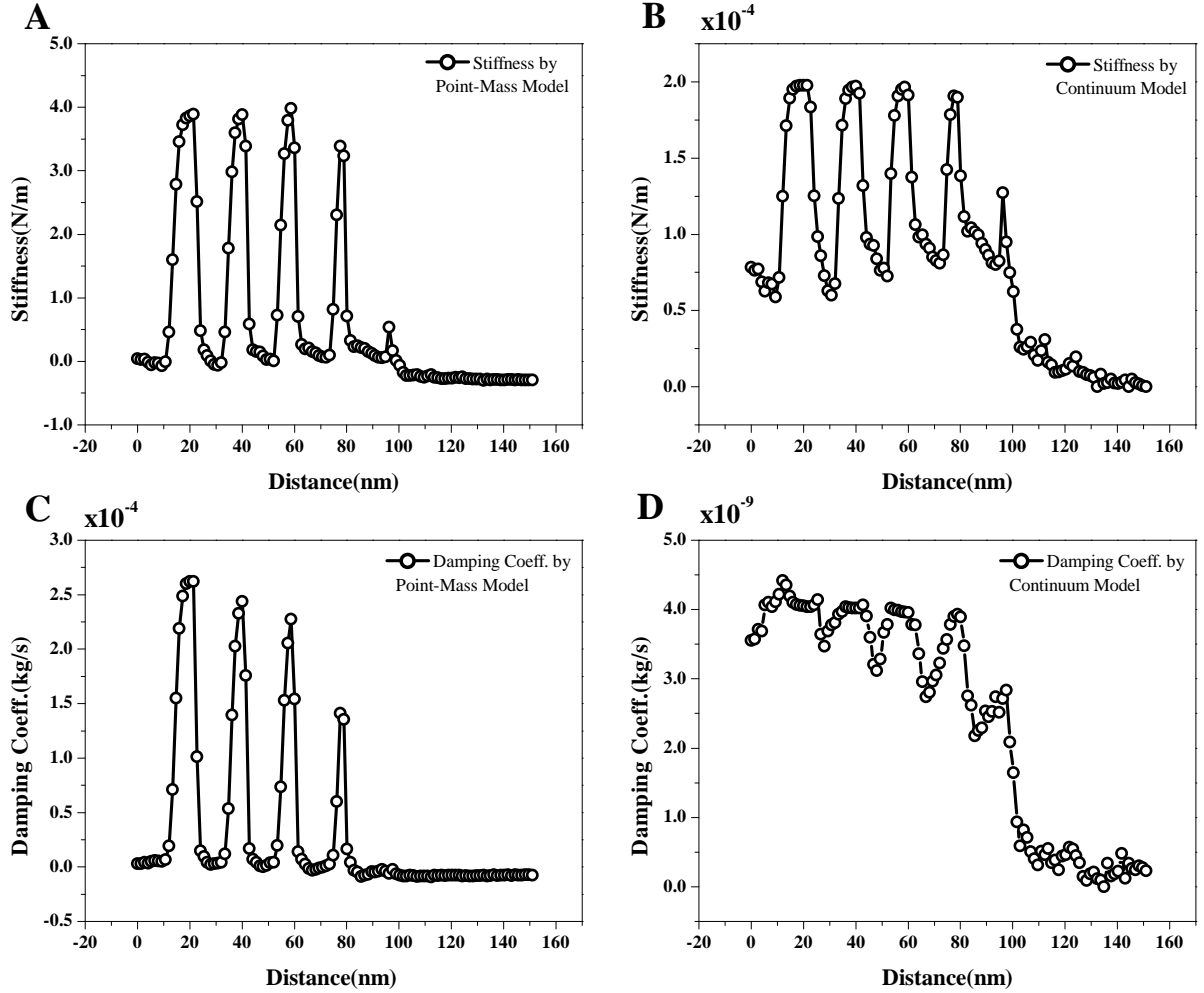


Figure 4.2: Shows The stiffness (a) and dissipation (c) calculated from amplitude and phase using point-mass model. We used equation 2.9 and 2.10 for this calculation. The point-mass model gives the stiffness in the range of few N/m and the dissipation as $\sim 10^{-4}$ kg/s. This is over 4 magnitudes higher than theoretical expectations. (b) shows the stiffness using equation 2.11 and and (d) shows the dissipation calculated using 2.12. The data in figure 3(c) and (d) is used for the calculations. The peak stiffness is 2×10^{-4} N/m and the dissipation is $\sim 10^{-9}$ kg/s

peak value of 4.5×10^{-9} kg/s. This value is over two magnitudes lower than the upper bound calculated from the non-observation by Benedetti et.al.

The analysis clearly suggests that the method proposed by Benedetti et.al is successful over the point-mass model for measurement of stiffness and dissipation of single proteins in liquid environments, provided a better detection system for sensing cantilever displacements is made.

4.2 Noise analysis

Since we are able to measure the stiffness and dissipation, in this section, we show the determination of the minimum detectable stiffness and dissipation of our instrument. In other words, the least count of the enhanced interferometric detection method. The method is based on measurement of powers in the noise floor at the frequency of operation. We can calculate the minimum detectable X and Y signal from the lock-in amplifier at the measurement bandwidth and propagate the errors in the equations 2.11 2.12. Figure 4.3 shows the power spectral density(PSD) of the thermally driven cantilever vibrations. The time-series data is collected for 1 s with 1 MHz sampling rate. The PSD correctly shows the thermal peak at the cantilever resonance of 12.9 KHz in water. (The thermal peak in the air is 32.42 KHZ). The noise floor at our operation frequency of 2KHz is $0.5 \times 10^{-2} \text{ \AA} / \sqrt{\text{Hz}}$. With the measurement bandwidth of 100 Hz decided by the Lock-in amplifier time constant, the maximum noise floor observed at 2 KHz is roughly $5 \times 10^{-2} \text{ \AA}$.

Note that the measurement now is limited by the thermal noise and hence increasing the sensitivity of interferometer wont help. This suggests that the minimum detectable X and Y are of the order $5 \times 10^{-2} \text{ \AA}$. Using error propagation in X and Y in equations (cite equations), the errors in stiffness and dissipation can be determined. We find the minimum detectable stiffness to be $\Delta k_i = 10^{-6} \text{ N/m}$ and the minimum detectable dissipation to be $\Delta \gamma_i = 10^{-11} \text{ kg/s}$.

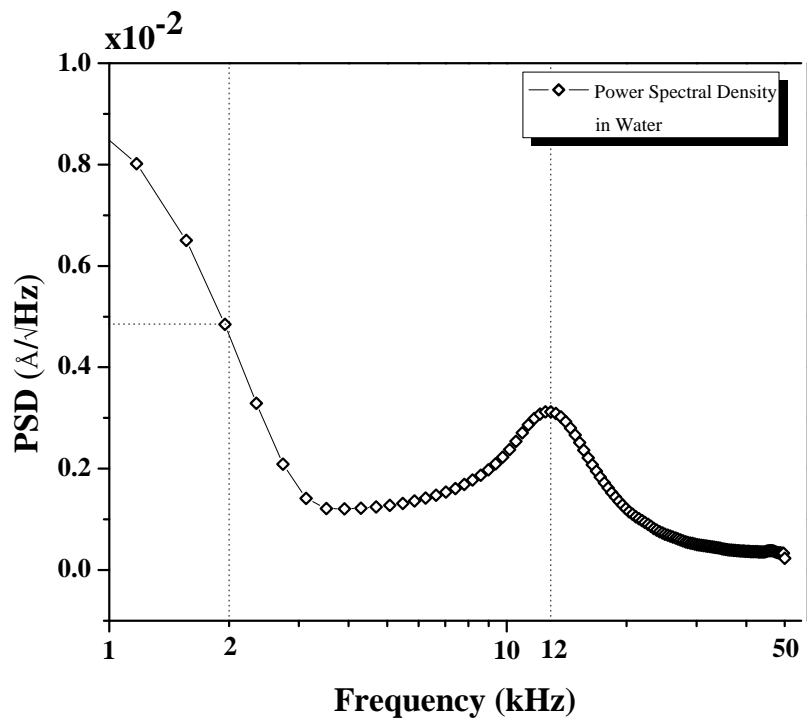


Figure 4.3: Power Spectral Density of thermally driven cantilever. The peak at 12:9 kHz is cantilever resonance. The minimum detectable stiffness and dissipation is estimated using the noise floor around 2 kHz.

Chapter 5

Discussion

In this chapter I will discuss how we can interpret the results in previous chapter and relate them to the physical picture of a protein molecule.

5.1 Origins of Elasticity and Dissipation in Proteins

We measured the stiffness and dissipation of an unfolding molecule as shown in chapter 4. In order to relate this to a physical picture, it is worthwhile to deliberate the origins of this viscoelastic response.

Stiffness: Stiffness, in general, is defined as the ability of a material to resist deformation. In most solids, stiffness or rigidity is a material property which arises from the stiffness of the individual bonds that hold the constituent atoms together. In proteins however, there are strong covalent bonds as well as weak physical bonds (electrostatic, hydrogen bonds and Van der Waals bonds). Flexible proteins such as titin resist deformation for a completely different reason. The deformations to the native structure during pulling tend to align the constituent polymeric chains. This alignment in thermodynamic sense can be seen as loss of entropy and is thus energetically unfavourable. Thus there is a resistance to the deformation that has entropic origins. This is true for all polymers and is referred to as Entropic Elasticity. A common example of this phenomenon is the rubber.

Dissipation: Dissipation in proteins arises due to two components, the solvent viscosity and the internal friction. The solvent viscosity is responsible for the hydrodynamic drag acting on the protein thus slowing down the movement of the molecule. Internal friction in the proteins is said to arise because the sliding of constituents in the protein structure past each other can be seen as breaking and formation of numerous weak bonds. Thus, one expects the protein movement or the shape change will be slowed down by this *internal viscosity* or *internal friction*. It has been shown in case of myoglobin that the protein friction is four times greater than the solvent viscosity (Ansari et. al. 1992)[23].

5.2 Thermodynamics of Protein Function

We discussed the origins of the viscoelastic response of the proteins in above section. Now, we will discuss how relevant this mechanical response is to protein function. A protein molecule carries out its function by changing its conformation which can be represented by a two-state process. There is a free energy barrier which needs to be overcome by the native state in order to go into the *active* state. Logically, one can argue that the protein must go over this barrier hence indicating a transition state of protein conformation. However, it should be noted that the process is different than a chemical reaction. Configuration change is a global change for a protein molecule which involves numerous making and breaking of non-specific bonds unlike simple chemical reaction. Hence, the transition state theory doesn't help in understanding protein function.

Considering a global configuration change, a more physically realistic model is given by Kramer's theory[24]. According to this model, the free energy barrier is overcome by a protein by diffusing into the barrier. The rate of this diffusion is represented by the inverse of the relaxation time which, is the ratio of the dissipative and the elastic modulus of the protein. $\tau = \gamma/k$. We can think of this from the frame of protein where it samples different points on the energy landscape every τ seconds where, τ is the time over which the configuration of the protein becomes statistically uncorrelated and we can say that protein has undergone a conformational change. The protein will react once it attains a configuration having free energy equal to the transition energy. This theory has been experimentally used to model myosin (Eisenberg and Hill, 1978)[25] and to study dynamics of conformation changes of proteins by (Ansari et. al. 1992)[23].

Thus, the kinetics of protein's conformational change is determined by the local relaxation time corresponding to the configuration changes of the molecule. The local relaxation time depends on the local stiffness and dissipation corresponding to the configuration. There are very few techniques to measure the direct and local viscoelastic response of single proteins. Thus, work carried out in this project is a step forward in the direction of understanding global slope change in protein to perform numerous biochemical tasks.

Figure 5.1 shows the relaxation time i.e ratio of the dissipation and stiffness calculated in Figure 4.2 (d) and (c) respectively.

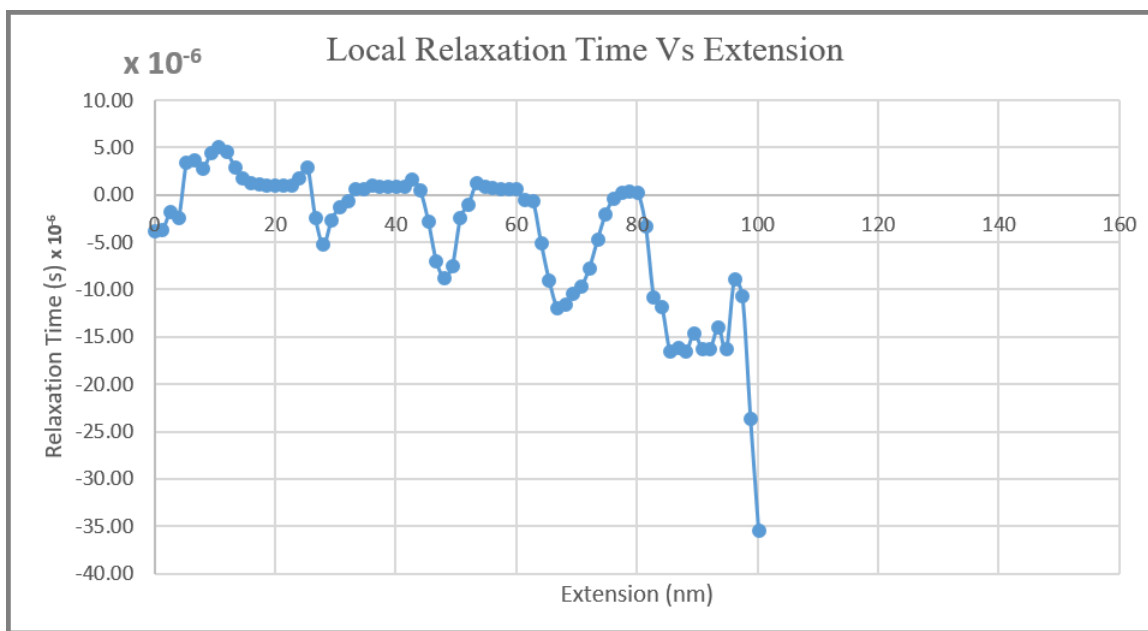


Figure 5.1: The local relaxation time calculated by taking the ratio of local dissipation and the stiffness shown in figure 4.2 $\tau = \gamma/k$

5.3 Future Plans

We saw in figure 5.1 the trend in the relaxation time changes as the protein unfolds. We need to understand its physical interpretation. The measurement reveals the stiffness and damping at a particular frequency. However, it will be interesting to study the unfolding behaviour at different excitation frequencies in the range of 100 Hz to 10 KHz which can give further insights into the time scales of different processes during protein unfolding. Other parameters like the excitation amplitude and pulling rates can also be explored. It is in fact important to sample this parameter space and observe the change in the unfolding behaviour.

The instrument can be improvised by implementing a robust acoustic shielding around it. The cantilever holder is suspected to contribute to some noise which needs to be addressed. With minor improvisations, one can implement a *force clamp* mechanism which has tremendous use in protein studies. This instrument yields fundamental stiffness and dissipation measurements and thus can be used for experiments on different systems such as lipid bilayers, polysaccharides or synthetic polymers.

Bibliography

- [1] B. Weber, “Life,” in *The Stanford Encyclopedia of Philosophy* (E. N. Zalta, ed.), Metaphysics Research Lab, Stanford University, spring 2015 ed., 2015.
- [2] Wikipedia, “What is life? — wikipedia, the free encyclopedia,” 2017. [Online; accessed 15-March-2017].
- [3] Wikipedia, “Biophysics — wikipedia, the free encyclopedia,” 2017. [Online; accessed 15-March-2017].
- [4] H. Chick and C. Martin, “On the heat coagulation of proteins: Part iv. the conditions controlling the agglutination of proteins already acted upon by hot water,” *The Journal of physiology*, vol. 45, no. 4, p. 261, 1912.
- [5] M. Anson and A. Mirsky, “Protein coagulation and its reversal: the preparation of insoluble globin, soluble globin and heme,” *The Journal of general physiology*, vol. 13, no. 4, p. 469, 1930.
- [6] C. B. Anfinsen, “Studies on the principles that govern the folding of protein chains,” 1972.
- [7] J. T. Edsall, “Hsien wu and the first theory of protein denaturation (1931),” *Advances in protein chemistry*, vol. 46, pp. 1–5, 1995.
- [8] K. A. Dill and J. L. MacCallum, “The protein-folding problem, 50 years on,” *Science*, vol. 338, no. 6110, pp. 1042–1046, 2012.
- [9] S. E. Radford, “Protein folding: progress made and promises ahead,” *Trends in biochemical sciences*, vol. 25, no. 12, pp. 611–618, 2000.
- [10] M. S. Kellermayer, S. B. Smith, H. L. Granzier, and C. Bustamante, “Folding-unfolding transitions in single titin molecules characterized with laser tweezers,” *Science*, vol. 276, no. 5315, pp. 1112–1116, 1997.
- [11] M. Rief, M. Gautel, F. Oesterhelt, J. M. Fernandez, and H. E. Gaub, “Reversible unfolding of individual titin immunoglobulin domains by afm,” *science*, vol. 276, no. 5315, pp. 1109–1112, 1997.

- [12] R. B. Best and J. Clarke, “What can atomic force microscopy tell us about protein folding?,” *Chemical Communications*, no. 3, pp. 183–192, 2002.
- [13] B. S. Khatri, M. Kawakami, K. Byrne, D. A. Smith, and T. C. McLeish, “Entropy and barrier-controlled fluctuations determine conformational viscoelasticity of single biomolecules,” *Biophysical journal*, vol. 92, no. 6, pp. 1825–1835, 2007.
- [14] C. A. Bippes, A. D. Humphris, M. Stark, D. J. Müller, and H. Janovjak, “Direct measurement of single-molecule visco-elasticity in atomic force microscope force-extension experiments,” *European Biophysics Journal*, vol. 35, no. 3, pp. 287–292, 2006.
- [15] P. Hinterdorfer, F. Kienberger, A. Raab, H. J. Gruber, W. Baumgartner, G. Kada, C. Riener, S. Wielert-Badt, C. Borken, and H. Schindler, “Poly (ethylene glycol): An ideal spacer for molecular recognition force microscopy/spectroscopy.,” *Single Molecules*, vol. 1, no. 2, pp. 99–103, 2000.
- [16] L. A. Chtcheglova, G. T. Shubeita, S. K. Sekatskii, and G. Dietler, “Force spectroscopy with a small dithering of afm tip: a method of direct and continuous measurement of the spring constant of single molecules and molecular complexes,” *Biophysical journal*, vol. 86, no. 2, pp. 1177–1184, 2004.
- [17] T. Okajima, H. Arakawa, M. T. Alam, H. Sekiguchi, and A. Ikai, “Dynamics of a partially stretched protein molecule studied using an atomic force microscope,” *Biophysical chemistry*, vol. 107, no. 1, pp. 51–61, 2004.
- [18] P. M. Hoffmann, S. Patil, G. Matei, A. Tanulku, R. Grimble, Ö. Özer, S. Jeffery, A. Oral, and J. Pethica, “Linear measurements of nanomechanical phenomena using small-amplitude afm,” in *MRS Proceedings*, vol. 838, pp. O1–8, Cambridge Univ Press, 2004.
- [19] F. Benedetti, Y. Gazizova, A. J. Kulik, P. E. Marszalek, D. V. Klimov, G. Dietler, and S. K. Sekatskii, “Can dissipative properties of single molecules be extracted from a force spectroscopy experiment?,” *Biophysical Journal*, vol. 111, no. 6, pp. 1163–1172, 2016.
- [20] V. Subba-Rao, C. Sudakar, J. Esmacher, M. Pantea, R. Naik, and P. M. Hoffmann, “Improving a high-resolution fiber-optic interferometer through deposition of a tio 2 reflective coating by simple dip-coating,” *Review of Scientific Instruments*, vol. 80, no. 11, p. 115104, 2009.
- [21] A. Steward, J. L. Toca-Herrera, and J. Clarke, “Versatile cloning system for construction of multimeric proteins for use in atomic force microscopy,” *Protein Science*, vol. 11, no. 9, pp. 2179–2183, 2002.
- [22] J.-C. Meiners and S. R. Quake, “Femtonewton force spectroscopy of single extended dna molecules,” *Physical Review Letters*, vol. 84, no. 21, p. 5014, 2000.

- [23] A. Ansari, C. M. Jones, E. R. Henry, J. Hofrichter, and W. A. Eaton, “The role of solvent viscosity in the dynamics of protein conformational changes,” *Science*, vol. 256, no. 5065, pp. 1796–1798, 1992.
- [24] P. Hänggi, P. Talkner, and M. Borkovec, “Reaction-rate theory: fifty years after kramers,” *Reviews of modern physics*, vol. 62, no. 2, p. 251, 1990.
- [25] E. Eisenberg, T. L. Hill, and Y.-d. Chen, “Cross-bridge model of muscle contraction. quantitative analysis,” *Biophysical Journal*, vol. 29, no. 2, pp. 195–227, 1980.